Development of Numerical Model for Highly-Flowable Strain Hardening Fiber Reinforced Concrete (HF-SHFRC) Columns Subjected to Lateral Displacement Reversals and High Axial Loading Level

Wisena Perceka, Wen-Cheng Liao, and Li-Wei Tseng

Abstract Highly-flowable strain hardening fiber reinforced concrete (HF-SHFRC) is one of the advanced concrete material technologies. This material has good workability in the fresh state and exhibits strain-hardening and multiple cracking characteristics of high-performance fibre-reinforced cementitious composites (HPFRCC) in the hardened state. The use of steel fibers in a reinforced concrete column can replace the number of transverse reinforcement without reducing column strength and deformation capacity. Several experimental studies on the cyclic behavior of HF-SHFRC columns were carried out to capture the big picture of the feasibility study of steel fibers to substitute the transverse reinforcement. However, information regarding the numerical model of steel fibers reinforced concrete column, particularly column subjected to displacement reversals, is very limited. In this paper, an analytical macro model for HF-SHFRC columns subjected to lateral displacement reversals and high axial loading level is developed. The steel fibers are converted into transverse reinforcement in order to obtain equivalent confinement. In general, the cyclic behavior of the HF-SHFRC column could be predicted.

Keywords Toughness ratio · Equivalent confinement · Fiber effectiveness factor · Equivalent bond strength · Highly-flowable strain hardening fiber reinforced concrete (HF-SHFRC) · Buckling spring · Shear spring

W. Perceka (✉)
Parahyangan Catholic University, Bandung, West Java 40141, Indonesia
e-mail: wperceka@unpar.ac.id

W.-C. Liao · L.-W. Tseng
National Taiwan University, Taipei 10617, Taiwan

S. Belayutham et al. (eds.), *Proceedings of the 5th International Conference on Sustainable Civil Engineering Structures and Construction Materials*, Lecture Notes in Civil Engineering 215, https://doi.org/10.1007/978-981-16-7924-7_17

1 Introduction

By using high-strength concrete (HSC) with compressive strength of 70 MPa and high-strength steel (HSS) with yield stress of 685 MPa or greater, the member cross-section size and the volume of concrete and steel reinforcing bars for the entire building structure can be reduced [1]. Owing to lower water-to-cementitious materials ratio of the HSC, the concrete is more durable [2]. However, the brittle behavior of high strength reinforced concrete during fracturing is still a primary concern despite wide application in the construction industry. This failure behavior can be disastrous for countries located in moderate to high seismic region. Since earthquakes are frequent and unpredictable and consequently, structures must be constructed to meet minimum ductility standards [3].

Traditional techniques to increase the compressive strength and ductility of reinforced concrete columns rely on increasing the amount of transverse reinforcement in the column. However, constructability decreases due to increase of the amount of transverse reinforcement. Therefore, new materials are required to be applied to reinforced concrete structures in hopes of leading a reinforced concrete member to maintain design strength without associated losses in constructability. Previous studies showed that adding short and discontinuous steel fiber to reinforced concrete improved the ductile behavior of concrete [4, 5]. In steel fiber reinforced concrete (SFRC), the presence of steel fibers substituting the transverse reinforcement can replace the number of transverse reinforcement without reducing column strength and deformation capacity [5].

Additionally, during fracturing, the steel fibers serve a bridging role and provide more tensile strength during fracturing than solid concrete. This behavior inhibits the formation of fractures and distributes the fractures to other regions of the concrete member. Concrete fails once the steel fibers either break or are completely pulled out from the concrete. As the result, the fibers reduce early flaking of the thin outer cover and help preventing sudden catastrophic failure. On the other hand, the presence of steel fibers reduces the workability of fresh concrete. This obstacle may become barrier for extending the application of steel fibers to reinforced concrete structures. Therefore, for cast in place purpose, Liao et al. in 2017 proposed highly-flowable strain hardening fiber reinforced concrete (HF-SHFRC) [6].

Highly-flowable strain hardening fiber reinforced concrete (HF-SHFRC) is one of advanced concrete material technologies, where this material has good workability in the fresh state and exhibits strain-hardening and multiple cracking characteristics of high-performance fiber reinforced cementitious composites (HPFRCC) in the hardened state. The tensile strain-hardening behavior prevents concrete cover to experience spalling early after cracking. Several experimental studies on the cyclic behavior of HF-SHFRC columns were carried out to capture the big picture of the feasibility study of steel fibers to substitute the number of transverse reinforcement [7, 8]. Although the experimental results are available, to the authors' knowledge, information regarding the numerical model of steel fibers reinforced concrete column, particularly column subjected to displacement reversals (cyclic loading), is very

Fig. 1 Lateral deformation of a RC column due to: **a** flexural, **b** slip, **c** shear

limited. This paper is aimed at developing an analytical macro model to predict the cyclic behavior of the SFRC columns under high axial loading level. The finite element software (OpenSees) was used to build the model of SFRC column in order to observe the response of SFRC columns. During earthquake, the column undergoes deformation, which is comprised of three components; flexural deformations, reinforcement slip deformation, and shear deformations, as shown in Fig. 1. In this study, the analysis is focused on SFRC columns experiencing flexural or flexure-shear failure only.

2 Constructed Analytical Model

The Open System for Earthquake Engineering Simulation (OpenSees) is a software framework for simulating the seismic response of the structural and geotechnical system that has been developed as the computational platform for research on performance-based earthquake engineering at the Pacific Earthquake Engineering Research Center [9]. OpenSees library provides several element commands, where the force-based beam-column element is usually used for constructing a reinforced concrete beam or column. In addition, the beam or column element is combined in series with zero-length element, where this zero-length element depends on the spring behavior. In order to construct behavior of concrete and steel reinforcement, the uniaxial material command providing both monotonic and cyclic uniaxial material behavior can be used. Section flexural response is modeled using fiber section command. The modeling procedure in this study refers to a composed analytical model proposed by Liu et al. [10]. The double-curvature column may be reduced to the equivalent cantilever column. By referring to PEER structural database manual, Perceka in 2019 and Liao in 2010 reported that reducing double-curvature large-scale column model to equivalent cantilever could compare column behavior consistently for a wide range of the testing configuration [11, 12]. For a double-curvature column, the lateral deformation of the large-scale model is multiplied by half (1/2) since the length of the equivalent cantilever is half of the length of the large-scale double-curvature column. This is because the contra-flexure point of the double-curvature column is assumed to always occur at the half-length of the large-scale double-curvature column model [13]. For the lateral strength, the lateral strength of the equivalent cantilever remains the same as that of the large-scale double-curvature column

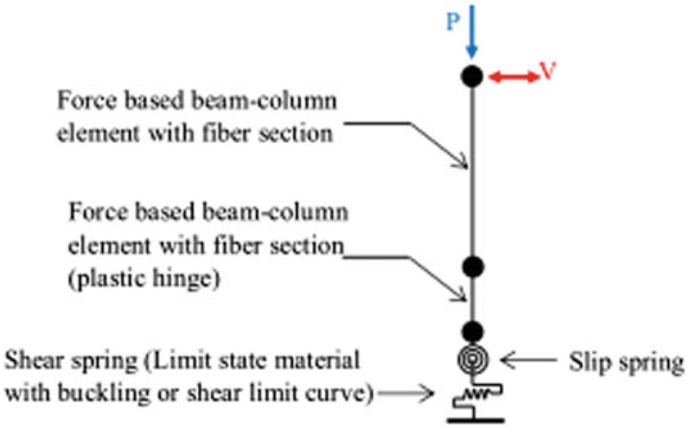

Fig. 2 A numerical model for SFRC column constructed by OpenSees

model. Figure 2 presents the analytical model of the column that is constructed in OpenSees (Fig. 2).

2.1 Forced-Based Beam-Column Element

The model of the column element is built using a force-based beam-column element. According to Teng et al. in 2016 [14], this element allows the nonlinear deformation of structural members in frames to be taken with a very coarse discretization. The forced-based beam-column element was used in the simulation of seismic performance of RC bridge columns, RC columns, or RC columns confined by fibre-reinforced polymer (FRP) in recent years [10, 14]. The force field is interpolated along with the element, as a result, element equilibrium is satisfied in a strict sense. For a member without distributed loads, typically, only one element is needed to perform a structural member in a frame. The Gauss–Lobatto integration scheme can be used, accordingly, since it has two integration points at the element ends where the maximum bending moments commonly occur. A schematic diagram of the five-point Gauss–Lobatto integration scheme for the sectional curvature of a cantilever column, which has also been shown by Teng et al. [14], is re-presented in Fig. 3.

2.2 Fiber Section

Fiber section is the section discretized based on fibers that collectively define section response. The stress–strain response of fibers is integrated to determine resultant behavior. A fiber section has a general geometric configuration formed by sub-regions

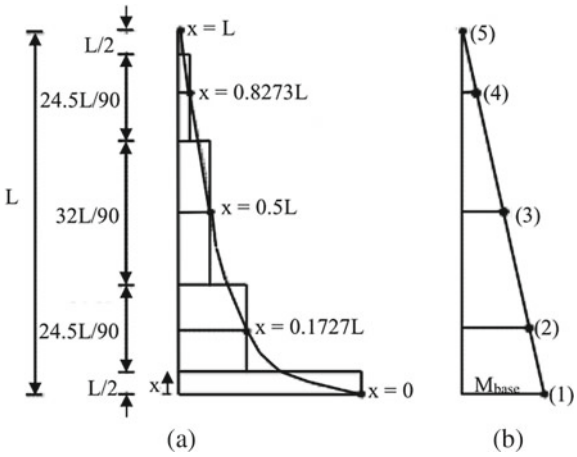

Fig. 3 The schematic diagram of the five-point Gauss–Lobatto for: **a** Curvature diagram, **b** Moment distribution for a force-based-beam-column element [14]

of simpler, regular shapes (quadrilateral, circular, and triangular regions), called patches. The steel reinforcement can be assigned by layer subcommand in order to construct the section of RC member.

2.3 Material Model

The fiber sections of concrete cover are assigned using the constitutive stress–strain model of concrete referring to 'Concrete04' and 'Concrete02', where this command is provided in uniaxial material command library. In order to show the steel fibers effect, the stress–strain model parameters of 'Concrete04' is defined based on the constitutive stress–strain model for steel fiber reinforced concrete in compression proposed by Liao et al. in 2015 [2]. Also, the parameters of tension part of 'Concrete04' are determined based on the constitutive stress–strain model for steel fiber reinforced concrete in tension proposed by Vianthy in 2015 [15]. The fiber sections of concrete core are assigned using the constitutive stress–strain model for confined concrete proposed by Cusson and Paultre [16]. The mechanical properties for confined concrete calculated by using Cusson and Paultre equation was assigned to 'Concrete04' to define behavior of column core. Since information regarding stress–strain model for confined concrete with steel fibers is very limited, the steel fibers shall be converted to transverse reinforcement. In 2016, Perceka et al. [4] proposed equations to calculate confinement efficiency of steel fiber reinforced concrete column confined by high strength transverse reinforcement. Those equations were proposed based on test results obtained from compression behavior of columns subjected to uniaxial concentric compression load. The confinement efficiency is expressed in term of toughness ratio that is the function of steel fiber and confinement parameters.

The 'Hysteretic' material model provided in uniaxial material command in OpenSees is selected to define the fiber sections of steel reinforcing bars. Liu et al. in 2014 performed iterative procedures to set the Pinchx and Pinchy parameters in the steel model [10]. It was reported that the Pinchx and Pinchy, respectively, were set as 0.5 and 0.4. Furthermore, it was reported that the post-yielding ratio of the steel should be adjusted to avoid negative stiffness in the beam-column element response and guarantee that a unique solution could be generated when the shear limit state material model was activated [10]. Also, the range of post-yielding ratio was varied from 0.5 to 2.5% of Young's modulus of steel [10]. In this study, the Pinchx and Pinchy are set as 0.5 and 0.4, respectively.

2.4 Spring in Zero-Length Element

It is worth mentioning that the behavior of the zero-length element depends on the spring behavior. Two zero-length elements are available at the bottom of column. Two different spring models are required to represent slip and shear behavior of the HF-SHFRC column, while flexural behavior depends on concrete and steel reinforcement materials assigned for beam-column element.

Rotational slip spring. The rotational slip spring was selected to consider the additional rigid body rotation that was caused by longitudinal reinforcement slip. The reinforcement slip is assumed to occur in tension reinforcement only. According to Liu et al. [10], the contribution of the bond-slip was kept to remain at the elastic level to conserve the model unpredictability. This approximation was selected after considering the high degree of nonlinearity in the proposed model. This elastic rotational stiffness can be determined using an equation proposed by Elwood and Eberhard in 2009 [17]. The rotational stiffness of slip spring, K_{slip}, is expressed in Eq. 1.

$$K_{slip} = \left[8.u/\left(d_{bl}.f_{yl}\right)\right].EI_{flex} \tag{1}$$

where d_{bl} is longitudinal reinforcement diameter, f_{yl} is longitudinal reinforcement yield stress, EI_{flex} is flexure stiffness of column section ($EI_{flex} = M_y/Ø_y$), u is the bond stress of embedded longitudinal bar, and d_{bl} is diameter of longitudinal reinforcement.

Buckling spring element. In order to simulate the behavior of HF-SHFRC columns experiencing flexural failure, the buckling spring is used. Similar to the analytical study conducted by Liu et al. [10], the buckling spring element shall be defined using the shear spring with the shear limit state proposed by Elwood [12]. Also, the nonphysical parameters of the spring, such as pinchx, pinchy, damage1, damage2, and beta can be set as 1.0, 1.0, 0.0, 0.0, 0.4, respectively [10]. In contrast, the pinchx and pinchy in this study are set as 0.5 and 0.4, respectively. Furthermore, Liu et al. [10] reported that the shear spring at the bar buckling failure point could be activated by shifting the original shear limit curve to the buckling point. The bar buckling limit, which is expressed as the ratio of delta-to-element length, can

be calculated using the equation proposed by Berry and Eberhard [18], as given in Eq. 2.

$$\Delta_{bb}/L\ (\%)\ =\ 3.25\,(1 + K_{ebb}.\rho_{eff}.d_{bl}/D).\left(1 - N_u/\left[A_g.f'_c\right]\right).(1 + L\ /\ 10D) \quad (2)$$

where Δ_{bb}/L is the drift ratio corresponding with the bar buckling failure, K_{ebb} is a coefficient that is equal to 40, 150, or 0 for rectangular-reinforced columns, spiral-reinforced columns, columns with a ratio of transverse reinforcement spacing-to-diameter of transverse reinforcement greater than 6, respectively, ρ_{eff} is a ratio of the volumetric transverse reinforcement ratio multiplied by the ratio of yield strength of transverse reinforcing bar-to-concrete compressive strength ($\rho_{eff} = \rho_s.f_{yt}/f'_c$), f_{yt} and f'_c, respectively, are the yield strength of transverse reinforcement and concrete compressive strength. Also, L is the distance from the one of column ends to the point of contra flexure, D is the column section depth, N_u is axial load acting on column cross-section, and A_g is the area of column cross-section.

Once the bar buckling failure is detected, the shear strength of the column decreases up to all shear strength capacity losses. The collapse displacement is adjusted to be twice displacement at bar buckling failure detected. Therefore, the degrading slope of the total response can be calculated using Eq. 3.

$$k^t_{deg} = V_u/(\Delta_c - \Delta_{bb})\ =\ V_u/\Delta_{bb} \quad (3)$$

The degrading slope of the shear spring response was empirically set as fifty percent of the degrading slope of the total response. Additionally, the symbol V_u in Eq. 3 denotes the shear strength of the column.

Shear spring element. It is known that as the displacement ductility decreased, shear failure governs. This condition causes the column to fail in shear prior to bar buckling. If the shear failure occurs after the yielding of longitudinal reinforcement, the failure mode is called flexure-shear failure. As mentioned, the bar buckling failure is calculated based on the original shear limit curve proposed by Elwood [18]. To simulate the HF-SHFRC column failing in flexure-shear, the shear limit curve is defined in Eq. 4.

$$\Delta_s/L\ = 3/100\ + 4\rho'' - v_u/\left(40.\mathrm{sqrt}\left(f'_c\right)\right) - N_u/\left(40.A_g.f'_c\right)\ \geq 1/100 \quad (4)$$

where $\Delta s/L$ is the drift ratio at shear failure, ρ'' is the transverse reinforcement ratio and v is the nominal shear stress that is the sum of shear strength provided by concrete and transverse reinforcement.

Like modeling for a column experiencing flexural failure, once the shear failure point is reached, the column's shear strength decreases until the column loses its shear capacity. According to Elwood [19], based on the intersection of total response and shear limit curve corresponding to detected shear failure, the degrading slope for the total response that is function of shear strength, displacement at shear failure detected, and displacement at axial failure detected, is expressed in Eq. 5.

$$k_{deg}^{t} = V_u/(\Delta_a - \Delta_s) \tag{5}$$

It shall be noted that Δ_a is displacement at axial failure, as given in Eq. 6.

$$\Delta_a/L = (4/100)\left(\left[1 + (\tan\theta)^2\right]/\left(\tan\theta + N_u.\left[s/\left(A_s.f_{yt}.d_c.\tan\theta\right)\right]\right)\right) \tag{6}$$

where d_c is the depth of the column core from the center line to center line of the ties, and s is the spacing of the transverse reinforcement.

2.5 Toughness Ratio

Toughness ratio, TR, is the ratio of the toughness of the concrete material or column under uniaxial compression to the toughness of the rigid material. Perceka et al. [4] described toughness as an area under the stress–strain or load-strain curve of SFRC column under uniaxial concentric load up to strain of 0.0154. Figure 4 presents the compressive stress–strain curve of the concrete material or column and that of rigid material. Perceka et al. [4] proposed a TR equation in term of transverse reinforcement and steel fiber parameters to quantify confinement efficiency of HF-SHFRC column under uniaxial compression by regressing 69 TRs of high strength concrete column without steel fibers and 27 TRs of high strength concrete column with steel fibers [2]. The TR of high strength concrete and HF-SHFRC column are given in Eqs. 7 and 8, respectively.

$$T_{R,HSC} = 0.48(T_{IT})^{0.18} \tag{7}$$

$$T_{R,HF-SHFRC} = 0.48(T_{IT} + 0.62T_{If})^{0.18} \tag{8}$$

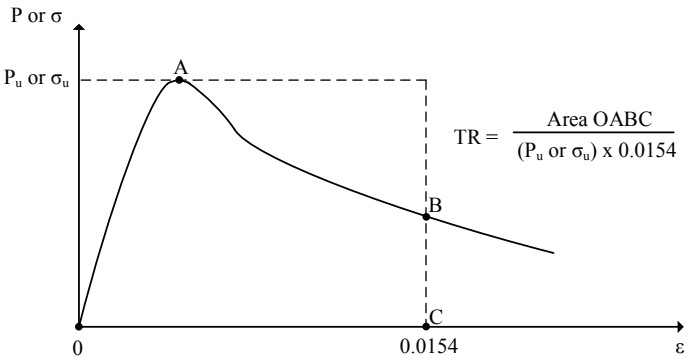

Fig. 4 Toughness ratio TR of RC column under uniaxial compression

where $T_{R,HSC}$ is TR of high strength concrete column, $T_{R,HF\text{-}SHFRC}$ is TR of high strength SFRC column, T_{It} is effective confinement index, and T_{If} is confinement index steel fibers. T_{It} and T_{If} are given in Eqs. 9 and 10, respectively.

$$T_{It} = k_e.\rho_s.f_{yt}/\left(f'_c.k_n\right) \tag{9}$$

$$T_{If} = V_f.(L_f/d_f).\tau_{eq}/f'_c \tag{10}$$

Equations 11 through 13 are provided to calculate the transverse reinforcement ratio in HF-SHFRC column.

$$\rho_s = 2A_{sh}/(s.b_c) \text{ (square column)} \tag{11}$$

$$\rho_s = \left[A_{shx}/(s.h_c) + A_{shy}/(s.b_c)\right] \text{ (rectangular column)} \tag{12}$$

$$k_n = n_l/(n_l - 2) \tag{13}$$

where A_{sh} is the total cross-section area of transverse reinforcement perpendicular to one direction, A_{shx} is the total cross-section area of transverse reinforcement perpendicular to the x-axis, A_{shy} is the total cross-section area of transverse reinforcement perpendicular to the y-axis, b_c is the side dimension of concrete core parallel to the x-axis, h_c is the side dimension of concrete core parallel to the y-axis, k_e is confinement effectiveness coefficient, k_n is confinement effectiveness factor, n_l is the number of longitudinal bars around the perimeter of the column core that are laterally supported by the corner of close-hoops or conventional ties having 135° hooks anchored into the concrete core, fyt is the yield stress of transverse reinforcement, V_f is fiber volume fraction, L_f is steel fiber length, d_f is steel fibers diameter, and τ_{eq} is the bond strength between steel fibers and the surrounding matrix.

The yield stress of transverse reinforcement for calculation shall not exceed 700 MPa. By using TR equation, the steel fibers can be treated as shear reinforcement, and the equivalent total shear reinforcement can be obtained.

2.6 Shear Strength Prediction Equation

Prior to this study, no equation is available for shear strength design or prediction of the steel fibers reinforced concrete column. Moreover, despite many shear strength equations proposed by other authors for designing or predicting the shear strength of a beam with steel fibers, no equation expresses concrete and steel fiber parameters in one term. Perceka et al. in 2019 [5] proposed an equation for predicting the shear strength of SFRC beam, where the concrete and steel fiber parameters are put in one

term. They also slightly modified the shear strength equation proposed in ACI 318–19 [20] by multiplying shear strength equation and fiber effectiveness factor. Since the equations for shear provided in ACI 318–19 [20] is applicable to both beam and column, the analytical shear strength of shear spring for HF-SHFRC column model can be predicted. Equations 14 and 15 are ACI equations that have been slightly modified by Perceka et al. [5]:

$$V_{c,SF} = \left[0.17\text{sqrt}\left(f'_c\right) + N_u/\left(6A_g\right)\right].F_{eff}.b_w.d \tag{14}$$

$$V_{c,SF} = \left[0.66(\rho_w)^{1/3} + N_u/\left(6A_g\right)\right].F_{eff}.b_w.d \tag{15}$$

where b_w is column section width, d is column effective depth, and ρ_w is the ratio of tension reinforcement, and F_{eff} is fiber effectiveness factor.

According to ACI 318–19 [20], if the amount of provided shear reinforcement is greater than the minimum requirement for shear reinforcement, either Eq. 14 or Eq. 15 can be used. For analysis and design, it is recommended to use the smallest of Eqs. 14 and 15. There are three equations for RC member provided in ACI 318–19 [20]; however, the third equation is provided for the reinforced concrete member with shear reinforcement less than the minimum requirement. The third equation is neglected in this study by assuming the fiber volume fraction of 0.75% equal to minimum reinforcement for SFRC beam. Equation 16 was proposed by Perceka et al. [15] to account for the fiber effectiveness factor that represents the steel fibers contribution in an SFRC beam.

$$F_{eff} = 1 + \left[\left(\tau_{eq}.V_f.L_f/d_f\right)/\left(0.75.\text{sqrt}\left(f'_c\right)\right)\right] \tag{16}$$

The shear strength provided by transverse reinforcement can be determined by using Eq. 17. As reported by Perceka in 2019 [12], in order to calculate the shear strength provided by high strength transverse reinforcement, the yield stress shall not be greater than 600 MPa.

$$V_s = A_v.f_{yt}.d/s \tag{17}$$

3 Benchmark Specimens

The selected column specimens that are referred to verify the numerical model constructed in this study are columns tested by Tseng in 2014 [21] and Perceka et al. in 2016 [3]. Table 1 and Fig. 5 present the parameters and section detailing for both specimens, respectively. Both S90-0.75 and S130-1.0 were made of HF-SHFRC material with specified concrete compressive strength of 100 MPa. However, the concrete compressive strength assigned in OpenSees is in accordance with the

Table 1 Parameters of HF-SHFRC column specimens

ID	$f'_{c,spec}$ [$f'_{c,test}$] in MPa (V_f [%])	longitudinal bars SD685 n_l-d_{bl} ($f_{y,test}$ [MPa])	Transverse bars SD785		$\frac{p}{A_g f'_c}$
			d_{bt} ($f_{y,test}$ [MPa])	S (mm)	
S90-0.75	100 [82.7] (0.75%)	8D32 (734), 8D25 (723)	D16 (816)	90	0.42
S130-1.00	100 [81.2] (1.00%)	8D32 (734), 8D25 (723)	D16 (816)	130	0.42

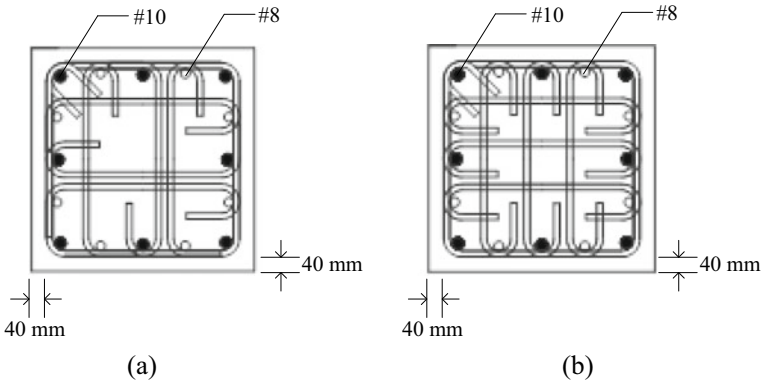

Fig. 5 Detail section for specimen: **a** S90-0.75 [21], **b** S130-1.0 [3]

compressive strength of cylinders tested on the same day with column specimens. The symbol S denotes column specimens, while two number following the S character denote transverse reinforcement spacing and fiber volume fraction, respectively. Those specimens were subjected to displacement reversals and a constant axial compression force ratio of 0.42.

Both specimens have the same cross-section design and similar longitudinal and transverse reinforcement layout. Specimen S90-0.75 has the transverse reinforcement with a single close hoop supporting longitudinal bars on the corners of the hoop and hooked end bent at 135° at one corner, crossties with a 90° at one end and 180° on the opposite end, and transverse reinforcement spacing of 90 mm. Unlike S90-0.75, specimen S130-1.0 has transverse reinforcement spacing of 130 mm, with all crossties having hooked end bend at 180° at both ends.

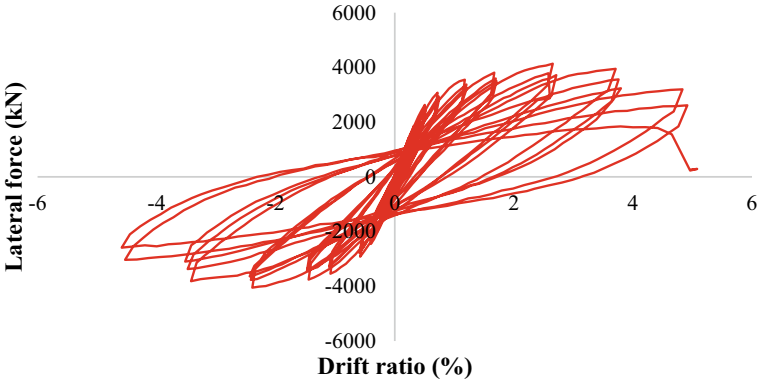

Fig. 6 The hysteresis loops for specimens S90-0.75 [21]

4 Benchmark Specimens

4.1 Specimen S90-0.75

In specimen S90-0.75, the transverse reinforcement with single close hoop supporting longitudinal bars on the corners of the hoop and having hooked end bent at 135° at one corner and crossties with a 90° at one and 180° on the opposite end. Both specimens were subjected to constant high axial compression force with an axial load ratio of 0.42. The hysteresis loops for specimens S90-0.75 is plotted in Fig. 6. The peak lateral strength was reached once the drift ratio was 2.65% that corresponded with the maximum lateral strength of 4135 kN. The ultimate drift ratio (UDR) (drift ratio corresponding to 80% maximum lateral capacity) of S90-0.75 was 4.23%, where the UDR was greater than 3%. Specimen S90-0.75 failed once the drift ratio was 4.59%.

4.2 Specimen S130-1.0

Like specimen S90-0.75, specimen S130-1.0 was subjected to constant axial compression force with an axial load ratio of 0.42. The transverse reinforcement spacing in S130-1.0 is one-fourth of effective column depth (d/4). Figure 7 presents the hysteresis loops for specimen S130-1.0. At a 1% drift ratio, the stiffness of specimen S130-1.0 began to decrease. The lateral strength and the corresponding drift ratio to peak strength were 3856.25 kN and 2.26%, respectively. The 3.78% drift ratio was reached once the ultimate strength dropped by about 20%. Therefore, the ultimate drift ratio was greater than the minimal acceptance drift ratio (3%). Notably, at a drift ratio of 4%, the lateral strength of the specimens rapidly decreased. Once a

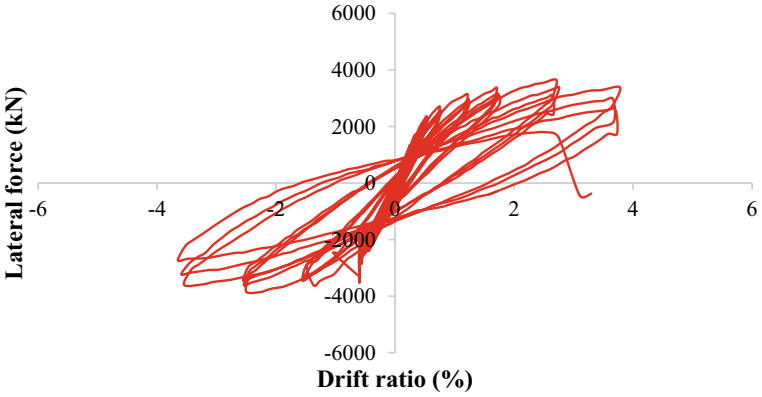

Fig. 7 The hysteresis loops for specimens S130-1.0 [3]

4% drift ratio was reached during the 3rd hysteresis loop, the specimen failed under axial loading.

5 Comparison Between Experimental and Numerical Model

Figures 8 and 9 present the comparison of experimental and predicted response of column tested by Tseng in 2014 [21] for S90-0.75 and Perceka et al. in 2016 for S130-1.0 [3]. As shown in both figures, the drift response for both experimental and numerical model is in the range of −4.5 to + 5.0%. From both experimental and numerical model, it can be known that the column was able to maintain the lateral

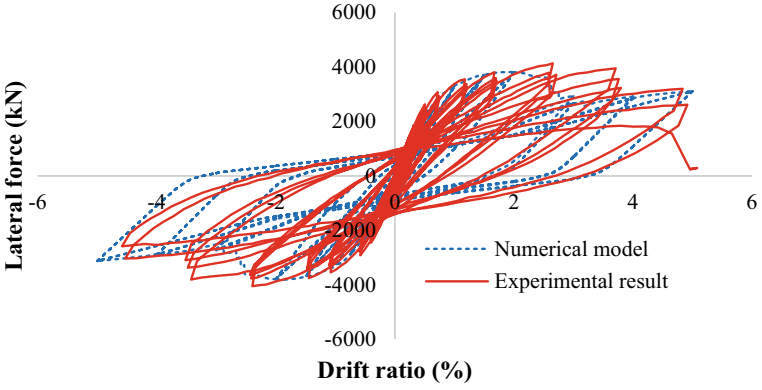

Fig. 8 Comparison between experimental and numerical model for specimen S90-0.75

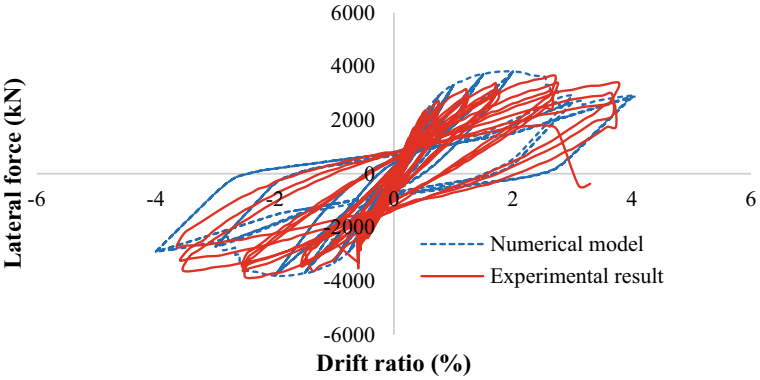

Fig. 9 Comparison between experimental and numerical model for specimen S130-1.0

strength at a large drift ratio, despite under high axial loading level. The maximum lateral strength of the numerical model for S90-0.75 was 3820 kN, where this value was slightly less than that of the experimental result. From a comparison between the experimental and numerical model for specimen S130-1.0, the difference between the experimental and numerical model for lateral strength was only 40.1 kN, where the lateral strength of experimental was slightly higher than that of the numerical model. The initial lateral stiffness of the numerical model for both specimens was almost similar to that of the experimental model. However, it can be seen in both comparison figures that the drift ratio corresponding to the peak strength of the experimental was greater than that of the numerical model. Since a numerical model for RC column consisted of beam-column element and buckling or shear spring, the column response highly depends on those elements. Once the shear failure in shear or buckling spring was detected, the degrading slope tended to follow the post-peak response of spring prior to degradation of the beam-column element. The response of slip of longitudinal reinforcement was assumed to be constant, while in the real test, the slip response affected the behavior of the column. In general, the hysteretic curves resulted from the numerical model can capture the peak strength and strength decay in columns. However, the overall response was not predicted well in many cycles.

6 Conclusions

An analytical macro model has been developed in order to simulate the cyclic behaviour of high strength concrete columns with high strength steel reinforcement and steel fibre. Since no stress–strain model for steel fibre concrete confined by high strength reinforcing is available, particularly high strength steel fibre reinforced concrete confined by high strength transverse reinforcement, the steel fibers shall be

converted into transverse reinforcement. Therefore, the equivalent confinement can be obtained. Once the equivalent transverse reinforcement is obtained, the parameters of the traditional stress–strain model for confined concrete can be adopted to develop a stress–strain curve based on uniaxial material "Conrete04" in OpenSees. Although the overall response could not be well predicted in many cycles, the hysteretic curves resulted from the numerical model could still capture the peak strength and strength decay in columns. Therefore, in general, the cyclic behavior of the HF-SHFRC column could still be predicted.

References

1. Lee HJ, Chen JH (2014) Testing of mechanical splices for grade 685 steel reinforcing bars. TTK Report, NCREE
2. Liao WC, Perceka W, Liu EJ (2015) Compressive stress-strain relationship of high strength steel fiber reinforced concrete. J Adv Concr Technol 13(8):378–392
3. Perceka W, Liao WC, Tseng LW (2016) Application of highly-flowable strain hardening fiber reinforced concrete in NEW RC Columns. In: Maekawa K, Kasuga A, Yamazaki J (eds) Proceeding of The 11th fib international PhD symposium in civil engineering. The University of Tokyo. Tokyo, Japan
4. Perceka W, Liao WC, Wang YD (2016) High strength concrete columns under axial compression load: hybrid confinement efficiency of high strength transverse reinforcement and steel fibers. Materials 9(4)
5. Perceka W, Liao WC, Wu YF (2019) Shear strength prediction equations and experimental study of high strength steel fiber reinforced concrete beams with different shear span-to-depth ratios. Appl Sci 9(22)
6. Liao WC, Perceka W, Yu LC (2017) Systematic mix procedures for highly flowable-strain hardening fiber reinforced concrete (HF-SHFRC) by using tensile strain hardening responses as performance criteria. Sci Adv Mater 9(7):1157–1168
7. Kimura H, Ishikawa Y, Kambayashi A, Takatsu H (2007) Seismic behavior 200 MPa ultra-high-strength steel-fiber reinforced concrete columns under varying axial load. J Adv Concr Technol 5(2):193–200
8. Lee HH (2007) Shear strength and behavior of steel fiber reinforced concrete columns under seismic loading. Eng Struct 9:1253–1262
9. OpenSees Homepage, https://opensees.berkeley.edu. Last Accessed 29 Apr 2020
10. Liu K, Witarto W, Chang K (2014) Composed analytical models for seismic assessment of reinforced concrete bridge columns. Earthq Eng Struct Dynam 44(2):265–281
11. Liao WC (2010) Performance-based plastic design of earthquake resistant reinforced concrete moment frames. PhD Dissertation. Department of Civil and Environmental Engineering, University of Michigan, Ann Arbor, Michigan
12. Perceka W (2019) Shear behavior of high strength steel fiber reinforced concrete columns. Doctoral Dissertation. College of Engineering-Department of Civil Engineering, National Taiwan University, Taiwan
13. Berry M, Parrish M, Eberhard M (2004) PEER structural performance database user's manual (Version 1.0)
14. Teng JG, Lam L, Lin G, Lu JY, Xiao QG (2016) Numerical simulation of FRC-jacketed RC columns subjected to cyclic and seismic loading. J Compos Constr 20(1)
15. Vianthy A (2015) Analytical study of shear capacity and behavior of highly flowable strain hardening steel fiber reinforced concrete panel. Master Thesis. College of Engineering-Department of Civil Engineering, National Taiwan University, Taiwan

16. Cusson D, Paultre P (1995) Stress-strain model for confined high-strength concrete. J Struct Eng 121(3):468–477
17. Elwood KJ, Eberhard MO (2009) Effective stiffness of reinforced concrete column. ACI Struct J 106(4):476–484
18. Elwood KJ (2004) Modelling failures in existing reinforced concrete columns. Can J Civ Eng 31:846–859
19. Berry M, Eberhard MO (2005) Practical performance model for bar buckling. J Struct Eng 131(7):1060–1070
20. ACI Committee 318 (2019) Building code requirement for structural concrete (ACI 318-19) and commentary. American Concrete Institute: Framington Hills, MI. USA
21. Tseng LW (2014) Feasibility study of steel fibers as a substitute for transverse reinforcement in new RC columns. Master Thesis. College of Engineering, Department of Civil Engineering, National Taiwan University, Taipei, Taiwan (2014). (In Chinese)